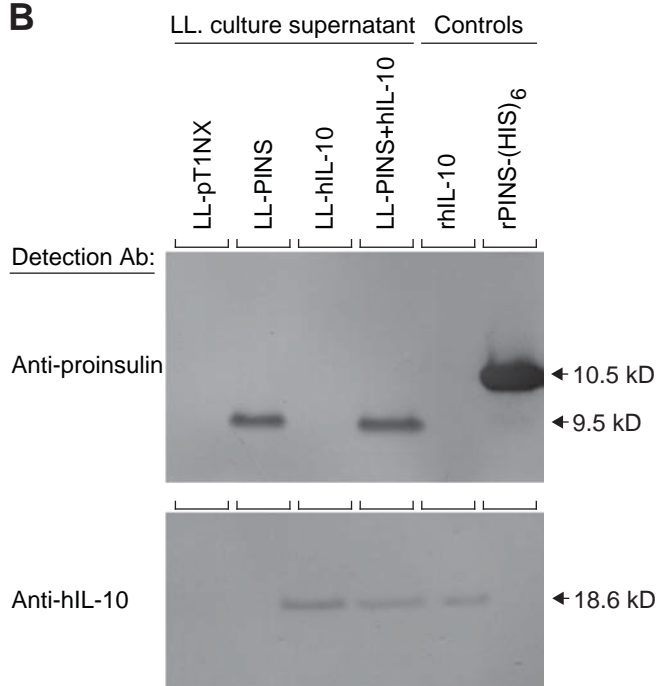


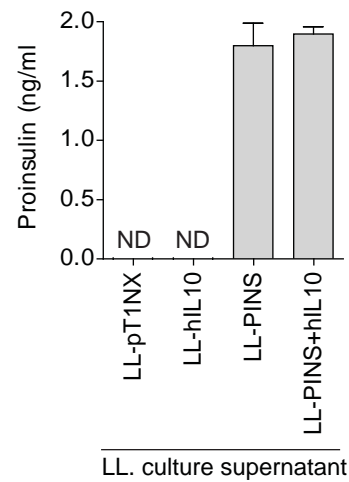
**A**

<i>L. lactis</i> strain	Common name	Cargo	Mode of production	Comments
MG1363	LL			Parental <i>L.lactis</i> strain
MG1363[pT1NX]	LL-pT1NX			Empty vector control strain
MG1363 [pThyAhPINS]	LL-PINS	hPINS	Plasmid-driven	MG1363 was genetically modified by inserting a plasmid carrying the hPINS gene
sAGX0037	LL-hIL10	hIL10	Genomically-integrated	MG1363 derivate containing the hIL10 expression cassette chromosomally integrated
sAGX0037 [pThyAhPINS]	LL-PINS+hIL10	hPINS and hIL10	Plasmid-driven (hPINS) Genomically-integrated (hIL10)	sAGX0037 was genetically modified by inserting a plasmid carrying the hPINS gene

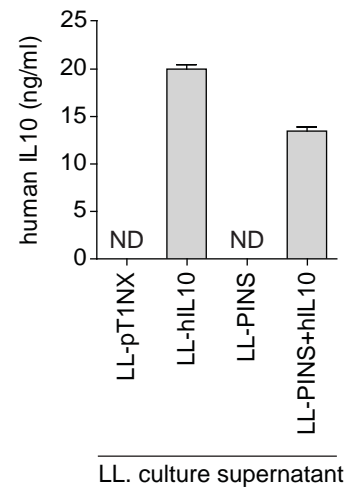
**B**

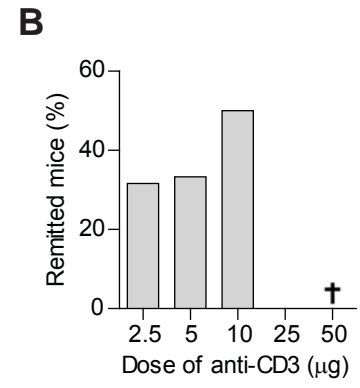
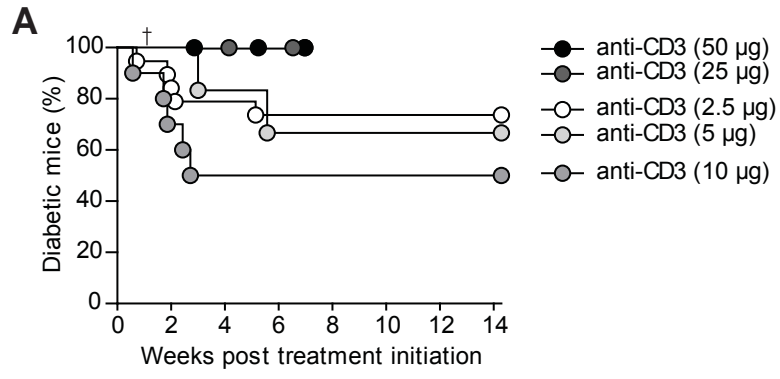


**C**

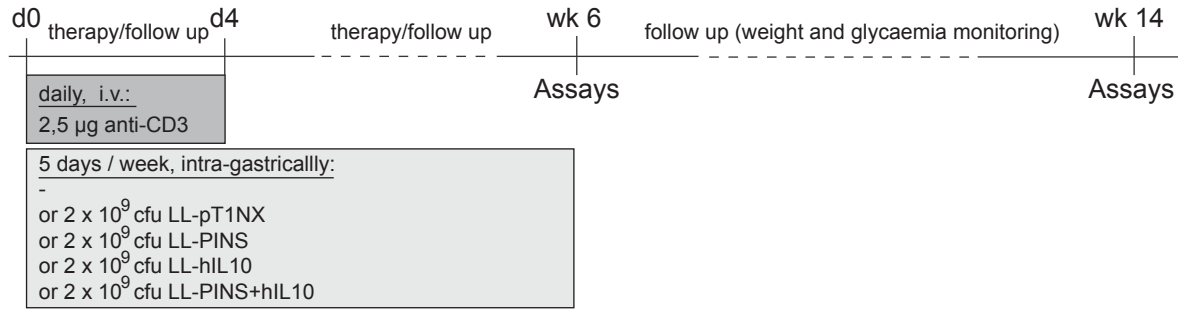


**D**

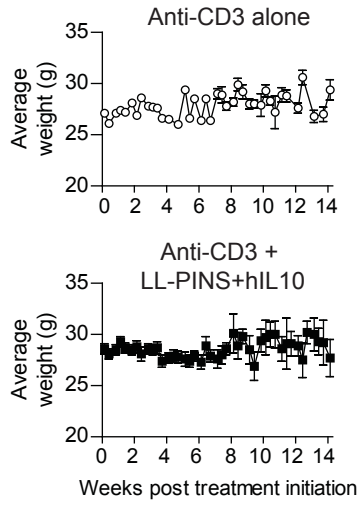




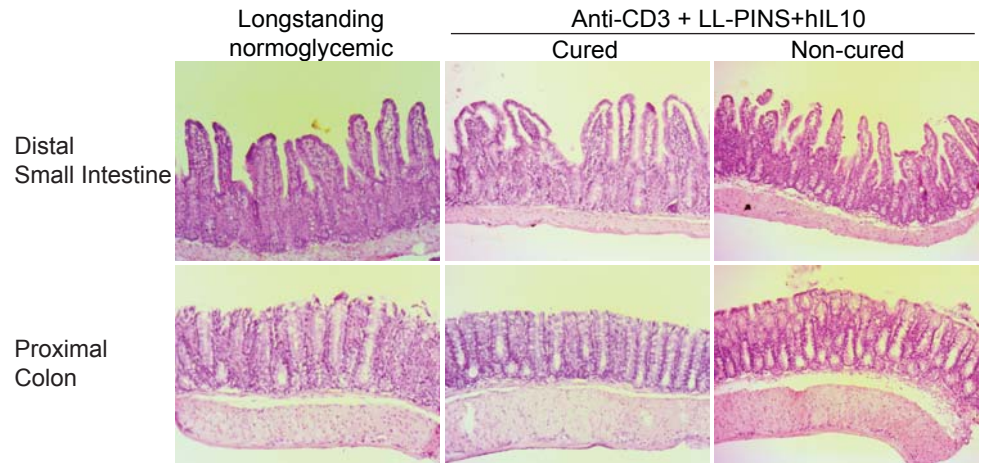
**A**



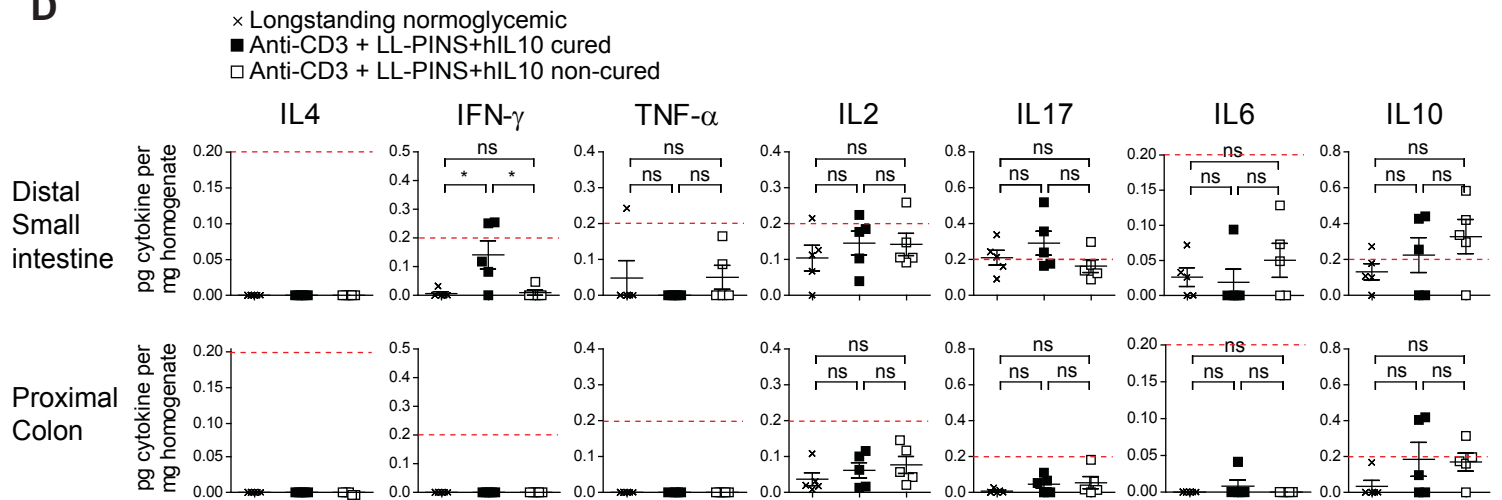
**B**

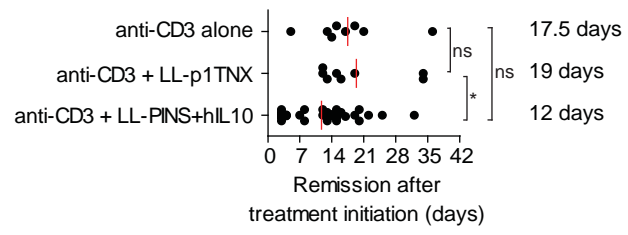


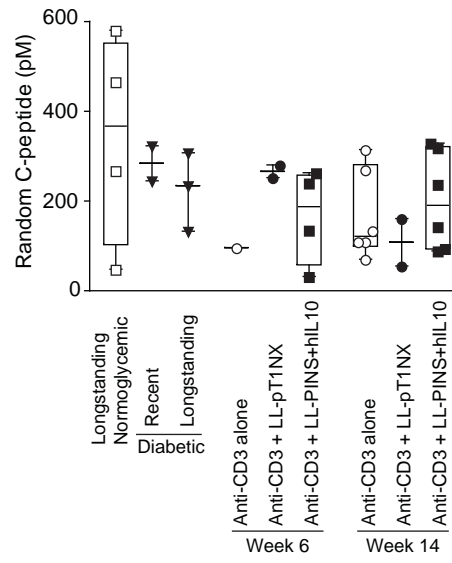
**C**

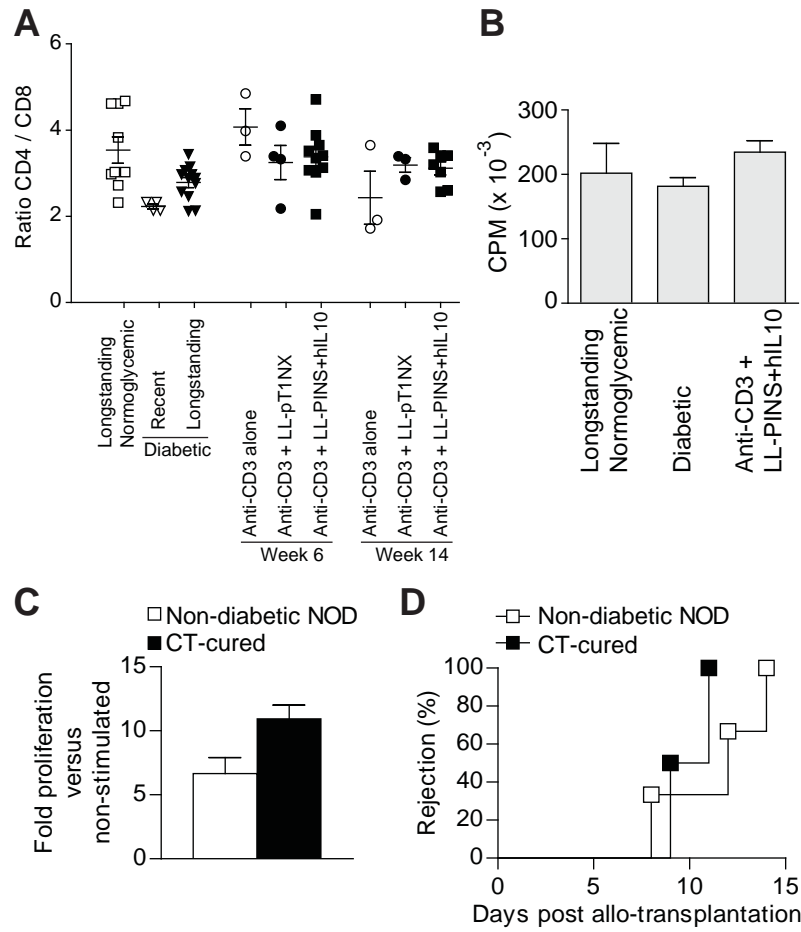


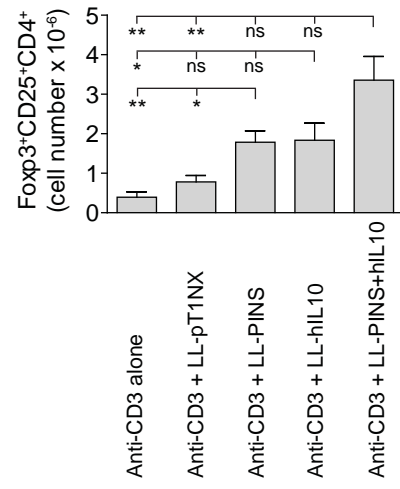
**D**

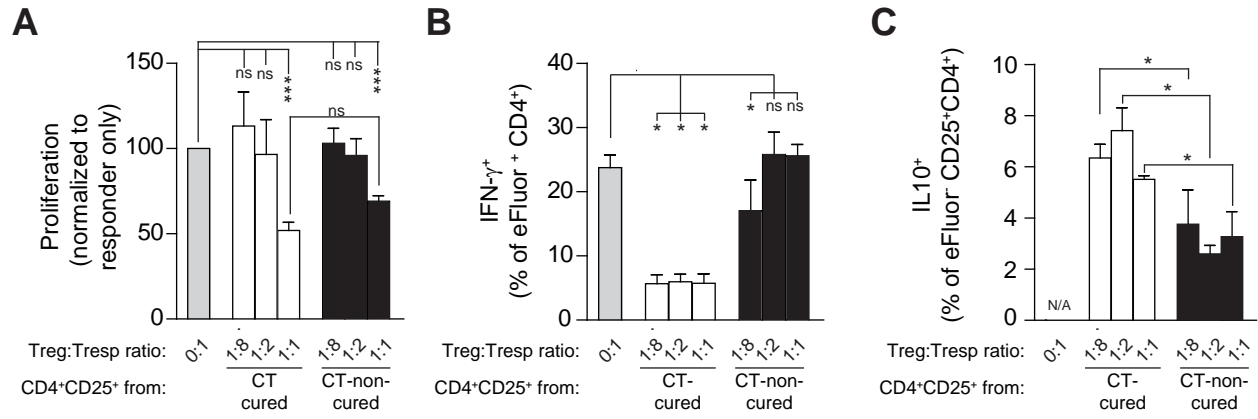




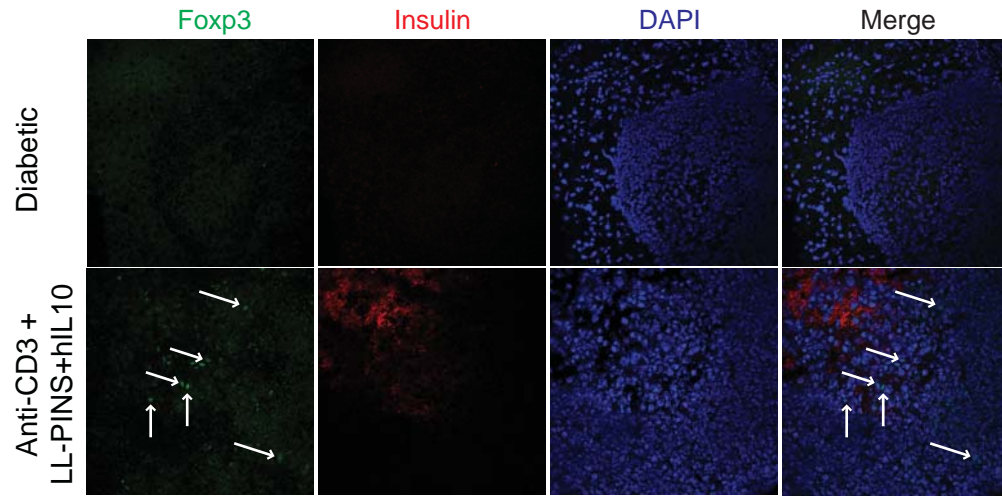


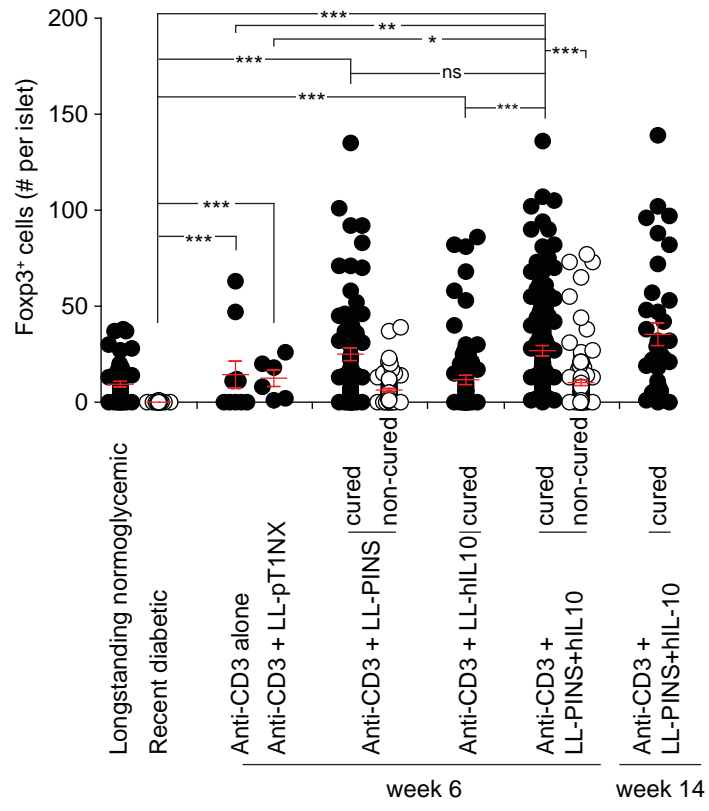












## Legends to supplemental Figures:

### Supplemental Figure 1.

GM *L. lactis* strains can secrete detectable amounts of full-size human PINS and/or IL10. **(A)** Overview of the *L.lactis* strains used in this study. **(B)** Western blots showing the presence of PINS (9.5kDa) and hIL10 (18.6kD) in the supernatant of the empty vector control (LL-pT1NX), LL-PINS, LL-hIL10, or LL-PINS+hIL10. Each lane on the blot represents 1 ml of *L. lactis* (LL.) culture supernatant. 50 ng of recombinant hPINS-(HIS)<sub>6</sub> (10.5 kD) and 50 ng of recombinant hIL10 (18.6 kD) were used as positive controls. **(C,D)** ELISA detection of PINS **(C)** and hIL10 **(D)** in the supernatant of indicated *L.lactis* strains. ND: Not detected.

### Supplemental Figure 2.

Dose-dependent diabetes reversal by anti-CD3 mono-therapy. Newly-diagnosed diabetic NOD mice were treated with different doses of FcR-binding anti-CD3 mAb in mono-therapy (145-2C11 clone; administered i.v. daily from day 0-4) as indicated. Glycemia was monitored. **(A)** Shown is the percentage of mice that remained diabetic after treatment. **(B)** Percentage of mice that were cured by week 6 after treatment initiation. †, dead or moribund mice.

### Supplemental Figure 3.

Combination therapy does not induce intestinal inflammation. **(A)** Schematic overview of the treatment regimens used in the study. **(B)** Average body weights of anti-CD3 mono-therapy (left panel) or CT with LL-PINS+hIL10 and anti-CD3 (right panel). **(C)** Photographs (×40) of HE-stained paraffin sections of a representative colon from normoglycemic and CT NOD mice. **(D)**

Production of the cytokines IL4, IFN- $\gamma$ , Tumor Necrosis Factor (TNF)- $\alpha$ , IL2, IL17, IL6, and IL10, as measured by cytometric bead array in the small intestine (top row) and colon (bottom row) of normoglycemic and CT NOD mice. Red dashed line indicates detection limit for reliable measurements. Statistical significance was calculated using Mann-Whitney non-parametric t-test (ns: not significant; \*  $P < 0.05$ ).

#### **Supplemental Figure 4.**

CT reverted autoimmune diabetes faster than anti-CD3 mono-therapy. Newly-diagnosed diabetic NOD mice received low-dose (2.5  $\mu\text{g}$ ) anti-CD3 mAb with or without *L.lactis* empty vector control (LL-pT1NX) or *L.lactis* LL-PINS+hIL10 and blood glucose levels were monitored. Symbols represent the individual day of remission, determined as the first day of stable normoglycemia. Line indicates the mean. d: days. Statistical significance was calculated using Mann-Whitney non-parametric t-test (ns: not significant, \*  $P < 0.05$ ).

#### **Supplemental Figure 5.**

Random C-peptide levels. Levels of unstimulated C-peptide were determined by ELISA in the serum of treated and control mice, as indicated. Shown are the individual values per mice overlaid with box and Tukey whisker plots.

#### **Supplemental Figure 6.**

Combination therapy conserves disease-irrelevant Teff responses. **(A)** At 6 and 14 weeks after treatment initiation, the frequencies of CD4<sup>+</sup> and CD8<sup>+</sup> T cells in the lymphocyte population were determined by flow cytometry of the spleens of treated and control mice, as indicated. Next, the CD4<sup>+</sup> over CD8<sup>+</sup> ratio was calculated and displayed as value per individual mice (symbol) and mean  $\pm$  s.e.m. (lines and cross-bars). **(B)** Proliferative response to PMA and ionomycin stimulation of splenocytes isolated from CT-cured mice after the 6 week treatment. Shown are the average  $\pm$  s.e.m. counts per minute (cpm) of a 3-day stimulation culture, with <sup>3</sup>H-thymidine added in the last 18 hours. **(C)** Mixed lymphocyte reaction (MLR) by splenocytes from non-diabetic NOD (open bar) or CT-cured (black bar) mice to C57BL/6 splenocytes. Displayed is the average fold proliferation  $\pm$  s.e.m. over non-stimulated NOD splenocytes, i.e. without C57BL/6 splenocytes. **(D)** *In vivo* allogeneic responses were determined by transplanting C57BL/6 skins onto non-diabetic NOD (open symbols, n = 3) or CT-cured NOD mice (black symbols, n = 2). Shown is the percentage of mice that rejected the third party graft.

### **Supplemental Figure 7.**

Combination therapy increases functional Tregs. Shown are the numbers of CD25<sup>+</sup>Foxp3<sup>+</sup>CD4<sup>+</sup> T cells in the spleen at 6 weeks after treatment initiation in diabetic NOD mice. Shown are averages  $\pm$  s.e.m. per group. Statistical significance was calculated using Mann-Whitney t-test (ns: not significant; \*  $P < 0.05$ , \*\*  $P < 0.01$ ).

### **Supplemental Figure 8.**

Tregs from CT-cured and CT-non-cured have similar *in vitro* polyclonal suppressive capacity despite differential influence on cytokine responses. CD4<sup>+</sup>CD25<sup>-</sup> responder T cells (Tresp) isolated from normoglycemic NOD were dye-labeled, stimulated using 0.1 μg/ml anti-CD3 and accessory cells for 72 hours in the presence of CD4<sup>+</sup>CD25<sup>+</sup> T cells (Tregs) isolated from cured or non-cured NOD mice at the end of combination therapy. **(A)** Proliferation of Tresp was measured by flow cytometry of dye dilution and shown as the percentage of Tresp undergone 2 or more divisions, normalized to Tresp only culture. **(B)** Activation of Tresp was assessed by intracellular cytokine staining (ICS) and flow cytometry for IFN-γ production and shown as percentage of CD4<sup>+</sup> Tresp (which were eFluor dye-labeled) positive for IFN-γ. **(C)** Production of IL10 by Tregs from CT-cured versus CT-non-cured NOD mice. Displayed is the percentage of CD4<sup>+</sup>CD25<sup>+</sup> Tregs (which were eFluor dye-negative) positive for IL10 by ICS and flow cytometry. Statistical significance was calculated using t-test (ns: not significant; \*  $P < 0.05$ , \*\*\*  $P < 0.001$ ).

### **Supplemental Figure 9.**

Immunofluorescence staining of Foxp3 and insulin in pancreatic sections. Pancreatic cyrosections from treated and control mice were subject to immunostaining for Foxp3 (green) and insulin (red), and nuclear staining with DAPI (blue), and used for Treg counting in **Figure 4B**. White arrows indicate Foxp3 positive cells.

### **Supplementary Figure 10.**

Local accumulation and autoAg-specific suppression by Tregs after combination therapy. Shown is the number of Foxp3-expressing cells in or around the pancreatic islets as determined by

manual counting of Foxp3<sup>+</sup> cells on immunostained cryosections as shown in **Supplementary Figure 7**. Statistical significance was calculated using Mann-Whitney t-test (ns: not significant, \*  $P < 0.05$ , \*\*  $P < 0.01$ , \*\*\*  $P < 0.001$ ).

## Supplemental Methods

*Construction of GM LL-PINS+hIL10* LL-PINS, an LL strain secreting human pro-insulin (PINS), was generated by transformation of the parenteral MG1363 strain with pThyAhPINS, a plasmid carrying PINS fused to the usp45 secretion signal, downstream of the PthyA lactococcal promoter. The DNA sequence encoding PINS was retrieved from GenBank (accession no. NC\_00011). LL-pT1NX is an MG1363 strain containing the empty vector pT1NX, and served as control. LL-hIL10, engineered to secrete human IL10 (hIL10), was generated by replacement of the chromosomally-located thyA expression cassette [PthyA>>thyA] in MG1363 strain by a hIL10 expression cassette [PhlIA>>SSusp45>>hIL10] as described<sup>17</sup>. LL-PINS+hIL10, an MG1363 strain secreting PINS along with hIL10, was generated by transformation of LL-hIL10 with pThyAhPINS (**Supplemental Figure 1A**).

*Bacteria and media* LL-hL10 was cultured in GM17T, i.e. M17 broth (BD, Franklin Lakes, NJ), supplemented with 0.5% glucose (Merck KGaA, Darmstadt, Germany) and 200 µM thymidine (Sigma, St. Louis, MO). Strains that were transformed with plasmids carrying PINS were cultured in GM17TE, i.e. GM17T supplemented with 5 µg/ml erythromycin (Sigma). Stock suspensions were stored at -80°C in 50% glycerol (Merck KGaA) in cryovials. For intragastric inoculations, stock suspensions were diluted 1000-fold in growth media and incubated for 16 h at 30°C, reaching a saturation density of  $2 \times 10^9$  cfu/ml. Bacteria were harvested by centrifugation and concentrated 10-fold in BM9 medium. Treatment doses consisted of 100 µl of this suspension.



*Quantification and verification of PINS and hIL10 secretion* To determine whether PINS and hIL10 were produced by recombinant *L.lactis* strains, immunoblotting and ELISA were performed. Proteins were separated on a 12% Bis-tris gel, and then transferred onto nitrocellulose membranes (dry blotting system, Invitrogen, Merelbeke, Belgium). The membranes were blocked, washed, and probed with either 1:500 diluted polyclonal antibody against PINS (Santa Cruz Biotechnology, Santa Cruz, CA) or 1:1000 diluted polyclonal antibody against hIL10 (BD Biosciences, Erembodegem, Belgium). Blots were washed and incubated with secondary antibodies diluted 1:1000, rabbit anti-goat AP or goat anti-rat AP respectively (Southern Biotech, Birmingham, AL). The reaction was developed by adding NBT/BCIP (Roche, Basel, Switzerland). 50 ng of recombinant human PINS-(HIS)<sub>6</sub> (kind gift of Luciano Vilella, Biommm S.A., Belo Horizonte, Brazil) and recombinant hIL10 served as positive controls. PINS levels were also determined using a commercial PINS ELISA (Merckodia, Uppsala, Sweden) according to the instructions of the manufacturer. This assay has a limit of detection of 4.5 pg/ml. hIL10 levels were determined using a sandwich ELISA developed and validated at ActoGeniX (Zwijnaarde (Ghent), Belgium). This assay is based on a rat anti-hIL10 antibody (BD Biosciences) as capture antibody and a biotinylated rat anti-hIL10 (BD Biosciences) in combination with Streptavidin-HRP as detection and has a lower limit of quantification of 5 pg/ml.

*Animals* NOD mice, originally obtained from Professor Wu (Department of Endocrinology, Peking Union Medical College Hospital, Beijing, China), were housed and inbred in animal facility of the Katholieke Universiteit Leuven since 1989. Housing of NOD mice occurred under semi-barrier conditions, and animals were fed sterile food and water *ad libitum*. NOD mice were

screened for the onset of diabetes by evaluating glucose levels in urine (Clinistix; Bayer Diagnostics, Tarrytown, NY) and venous blood (AccuChek, Roche). Mice were diagnosed as diabetic when having positive glucosuria and two consecutive blood glucose measurements exceeding 200 mg/dl. NOD/SCID and NOD/SCID  $\gamma c^{-/-}$  mice were bred from stocks purchased from the Jackson Laboratory (Bar Harbor, ME). Animals were maintained in accordance with the National Institutes of Health Guide for the Care and Use of Laboratory Animals, and all experimental procedures were approved and performed in accordance with the Ethics Committees of the Katholieke Universiteit Leuven (KUL, Leuven, Belgium) under project number 185-2009.

*Histology of pancreas and insulinitis grading* Six micron sections from formalin-fixed paraffin-embedded pancreata of each animal were cut and collected 100- $\mu$ m apart, then stained with hematoxylin eosin. Islets were observed under light microscopy at 20 $\times$  or 40 $\times$ , enumerated and graded by an independent investigator in blinded fashion. At least 25 islets per pancreatic sample were scored for islet infiltration as follows: 0, no infiltration; 1, peri-insulinitis; 2, islets with lymphocyte infiltration in less than 50% of the area, 3, islets with lymphocyte infiltration in more than 50% of the area or completely destroyed.

*Beta-cell proliferation* Sections from pancreata of CT-cured and longstanding normoglycemic and diabetic mice were double immunostained for insulin and the marker of replication Ki67. Briefly, sections were incubated for 1 h with guinea pig anti-swine insulin (DakoCytomation, Glostrup, DK; 0.3 mg/ml) diluted in PBS containing 3% BSA, followed by 1 h incubation with Alexa Fluor-488 conjugated goat anti-guinea pig secondary Ab (Invitrogen, Molecular Probes,

Carlsbad, CA; 4 µg/ml) diluted in PBS. The primary antibody for Ki67 (rabbit mAb, clone SP6, Thermo Scientific, Fremont, CA; 1:500) diluted in PBS contain 3% BSA was incubated for 30 min followed by 1 h of incubation with Alexa Fluor-594 conjugated goat anti-rabbit secondary Ab (Molecular Probes; 4 µg/ml). After nuclear staining with Hoechst 33342, slides were mounted with Vectashield mounting medium (Vector, Burlingame, CA, USA). Immunofluorescence-stained sections were analyzed with a Laser Confocal Microscope Leica TCS SP5.

All beta cells per pancreatic section (at least 4 sections per animal) were examined in details at 630× magnification (63× objective, 10× ocular) for the frequency of beta-cell replication as fractional Ki67 and insulin-positive cells. Beta-cell proliferation was quantified as (the number of insulin-positive/Ki67-positive cells of the 4 different sections / total number of insulin-positive cells per section) × 100. At least 7 islets were counted for each mouse.

*Flow cytometric analysis* Single cell suspensions of spleen and PLN were prepared at 6 and 14 weeks after treatment initiation. Cells were stained with directly conjugated Abs against CD4 (GK1.5), CD8a (53-6.7), CD25 (PC61.5), FR4 (eBio12A5) and matching isotype controls (all eBioscience). Intracellular staining (ICS) Abs against IFN-γ, IL10, Foxp3 and CTLA-4 or matching isotype controls were from eBioscience and used according to the manufacturer's instructions. Cells were analyzed in a FACSCanto™ flow cytometer with FACSDiva software (BD Biosciences).

*In vitro (Ag-specific) suppression and cytokine assay* CD4<sup>+</sup>CD25<sup>-</sup> Tresp, isolated from spleen and LNs of non-diabetic NODs (Dynabeads, Invitrogen, Merelbeke, Belgium), were labeled with

eFluor 670 Proliferation Dye (eBioscience). Splenic APCs from NOD/SCID  $\gamma c^{-/-}$  were used as accessory cells. Suppression assays were performed in round-bottom 96-well plates containing  $5 \times 10^4$  Tresp,  $1 \times 10^5$  accessory cells, in combination with either 0.5  $\mu\text{g/ml}$  or 0.1  $\mu\text{g/ml}$  soluble anti-CD3 mAb (clone 145-2C11, eBioscience), where indicated.  $\text{CD4}^+\text{CD25}^+$  T cells were isolated by a  $\text{CD4}^+$  enrichment-step followed by a  $\text{CD25}^+$ -selection step using the CellLection Biotin binder and bead removal kit (Dynabeads, Invitrogen, Merelbeke, Belgium).  $\text{CD4}^+\text{CD25}^+$  T cells isolated from anti-CD3- or CT-cured NOD mice, were used as putative suppressor cells at different ratio. After 72 h, flow cytometric analysis was used to determine proliferation via eFluor 670 Proliferation Dye dilution and activation via surface expression of CD69 (not shown) and CD44. Cell free supernatants were collected for detection of IFN- $\gamma$  and IL10 using a flowcytomix bead-based multiplex immunoassay (BenderMed Systems, eBioscience). The lower limit of detection for IFN- $\gamma$  and IL10 was 4.0 and 13.4 pg/ml, respectively.

To test Ag specificity of the suppression assay, eFluor 670 Proliferation Dye- labeled total  $\text{CD4}^+$  T cells, isolated from LNs and spleens of PINS- or OVA-immunized NOD mice (50  $\mu\text{g}$  CFA s.c. for 10 days), were used as Tresp. These cells ( $5 \times 10^4$  cells/well) were co-cultured in 96 well round bottom plates with  $1 \times 10^4$  cells per well thioglycolate-elicited APCs in the presence of 10  $\mu\text{g/ml}$  of autoAg (human PINS; kind gift of Luciano Vilella, Biommm S.A., Belo Horizonte, Brazil and Anthony Purcell, Molecular Science and Biotechnology Institute, Melbourne, Australia) or disease-irrelevant Ag (chicken OVA, grade V, Sigma-Aldrich, St. Louis, MO). After 96 hours, Tresp activation and proliferation in the presence or absence of  $\text{CD4}^+\text{CD25}^+$  T cells from CT-cured NOD mice, was determined as described above. In addition, analysis of IFN- $\gamma$  production by eFluor 670 $^+$   $\text{CD4}^+$  T cells and IL10-production by eFluor 670 $^-$   $\text{CD4}^+\text{CD25}^+$  T cells were assessed by means of intracellular flow cytometric analysis.

*Adoptive transfer of diabetes* Pooled splenocytes and PLN from treated NOD mice were assessed for their capacity to suppress the diabetogenic activity of splenocytes taken from an acutely diabetic donor. In brief, CD4<sup>+</sup>CD25<sup>+</sup> T-cells ( $1 \times 10^6$ ) isolated from 6-week CT-cured and CT-non-cured NOD mice were mixed with CD25-depleted splenocytes ( $1 \times 10^7$  cells) from female newly-diagnosed diabetic NOD mice and given i.v. into the tail veins of 6- to 8-week-old NOD/SCID mice. The mice receiving only  $1 \times 10^7$  CD25-depleted diabetic splenocytes were used as a positive control. The depleted cell population was evaluated for the presence of CD25<sup>+</sup> cells by flow cytometry; >95% of CD25<sup>+</sup> cells were removed by this procedure. Recipient mice were monitored twice weekly for the development of diabetes up to 50 days post-cell transfer.